J. Earth Syst. Sci. (2019) 128:134
https://doi.org/10.1007/s12040-019-1152-3

A study of frost occurrence and minimum temperatures in Iran

Batool Zeinali[1,*], Maryam Teymouri[1], Sayyad Asghari[1], Masiholah Mohammadi[1] and Vivek Gupta[2]

[1]*Faculty of Literature & Humanities, Department of Physical Geography, University of Mohaghegh Ardabili, Ardabil 09141549147, Iran.*
[2]*Department of Hydrology, Indian Institute of Technology Roorkee, Roorkee, India.*
**Corresponding author. e-mail: Zeynali.b@uma.ac.ir*

MS received 3 April 2018; revised 1 January 2019; accepted 13 January 2019; published online 14 May 2019

In this research, the frequency of frost is analysed from 95 synoptic stations for the period 1990–2015. This information was categorised by a fuzzy c-approach clustering algorithm and indicated that Iran is classified into five clusters with the aid of the frost-occurrence frequencies. The greatest frequency of days with frost prevalence is located in Cluster 1 that consists of Sarab station with an average annual frequency of 141.1 days over the period 1990–2015. The least frequent is found in Cluster 5 that consists of the stations positioned along the south and north coasts. Spatial association for the frequency of incidence of frost days also includes a dependence on elevation and latitude of stations, as well as their situation inside the course of external synoptic systems, bodily and geomorphological features and local climate. Also, a study of daily minimum temperature displays a widespread warming trend at some stage during this period, and has discovered an increase in the index of the number of tropical nights, warmest nights and coldest nights and decreasing trends have been determined in the number of frost days, cool nights and cold spell period index over most regions of Iran.

Keywords. Fuzzy clustering; frost occurrence; trend of minimum temperature; RClimDex; monitoring; climate change.

1. Introduction

In terms of climatology and meteorology, when the air temperature cools down and drops below 0°C, water vapour which comes into contact with cold surface gets converted into frost (Hejazizadeh and Naserzadeh 2007; Amer and Wang 2017). Frost is a primary climatological phenomenon which consists of temperature fluctuations that has changed over the years. It affects exceptional areas in numerous aspects, within unique latitudes, consistent with climatic zones and categories, and annually produces harmful losses in specific sections immediately or indirectly. Nearly every part of the economy may observe negative impacts with unexpected frost, and in most cases, the prevalence of frost has a poor effect (Rosenberg and Myers 1962). Frost has the largest effect on three economic areas: power, transport and agriculture, of which, the largest is the agriculture sector (Vega *et al.* 1994). Additionally, the most current Intergovernmental Panel on Climate Change (IPCC) report documented warming temperature traits on a global scale of 0.85°C (0.65−1.06°C), for the

period 1880–2012 (Hartmann *et al.* 2013; IPCC 2013; Crimp *et al.* 2016). Studies examining the nature of extreme minimum temperature occurrence (i.e., frost incidence) have predominantly been centred both on the regional and continental or global scales, with few local scale studies to date (Crimp *et al.* 2016). Consequently, it is very important to study the incidence of frost and trends of minimum temperature extremes. Frost is a primary environmental phenomenon internationally and in Iran.

The goal of this examination is mentioned in two parts: (i) to identify frost occurrence in Iran by fuzzy cluster analysis and (ii) to find and reveal the trend of the minimum temperatures using the RClimDex software program. Crimp *et al.* (2016) observed later seasonal and long-term changes in the southern Australian frost occurrence all through the period of 1960–2014 using extreme minimum temperatures. They recognised that the frost season length has increased on average approximately 26 days (in 2014) compared with the 1960–1990 long-term average. Also, the annual frequency of frost occurrence after August has increased by as much as four occurrences per year during the last decade, with localised increases of the incidence of the consecutive frost days also observed. Tamandani *et al.* (2015) mapped and analysed the threat of frost damage on horticultural vegetation in the Taftan location, in the southeast of Iran. The results showed that the earliest autumn frost and the latest spring frost occur in the Taftan Mountains, and the latest autumn frost and the earliest spring frost occur within the western and southeastern regions. Mahmoudi (2014) examined the use of multivariate regression trends, modelled the relationship among five statistical characteristics (i.e., the mean Julian day of the first frost, mean Julian day of the last frost, suggested range of frost days each year, the duration of the frost period and the average period of the growing season by way of three geo-climate elements: elevation, longitude and latitude). The results showed that the temperature of the highland regions which reached up to 4200 m above sea level was usually 0°C and colder throughout the year, and additionally, the coastal strip of southern Iran had no frost. Ghasemi and Khalili (2006, 2008) showed that Iran's temperature fluctuations, in particular, inside the northwest and west of the country, are strongly correlated with teleconnection patterns such as the Arctic oscillation (AO) and North Atlantic oscillation (NAO). Hernandez and Martinez (2009) examined the threat of the early and overdue below frost conditions of El Niño in Mexico, and, from examining the regression of frost periods and elevation, confirmed that the frost occurrence is more highly correlated with elevation than with El Niño. Mouhamed *et al.* (2013) evaluated the temperature and precipitation extremes over the West African Sahel. The results confirmed a well-known warming trend for the location during the period 1960–2010, specifically through an observable negative trend in cool nights, and more frequent warm days and warm spells. Parak *et al.* (2015) studied the traits and anomalies in everyday climate extremes in Iran over the period 1961–2010, and their results indicated a large and spatially coherent increase in temperature indices. Decreasing trends had been discovered in the diurnal temperature variations, cold spell period index and cool nights over most regions of Iran. Soltani *et al.* (2016) evaluated a climatology of extreme temperature and precipitation events over Iran. A warming trend in extreme temperatures was shown, with a large percentage of stations having statistically significant trends for all temperature indices. During the last 15 yr (1995–2010), the range of cold days and nights has decreased by way of 4 and 3 days/decade, respectively. The average annual mean, maximum and minimum temperatures throughout Iran increased by between 0.031° and 0.059°C per decade.

2. Materials and methods

2.1 *Case study*

The location of the study area (i.e., Iran) lies between 25°N and 40°N latitude and between 44°E and 64°E longitude with an elevation range of −28 to 5610 m (figure 1). Elburz and Zagros are the essential mountains of Iran, which play a vital function in the non-uniform spatio-temporal distribution of temperature and precipitation in Iran (Parak *et al.* 2015). The Caspian Sea is located in the northern region, supplying a maritime influence, even as the south is influenced by the Oman Sea and the Persian Gulf. The coastal Caspian Sea is typically moderate, humid and wet, with air temperatures rarely falling below 0°C or exceeding 29°C. Mountainous areas experience extreme winters and heavy snowfall, whereas the other regions are arid, with their humidity and

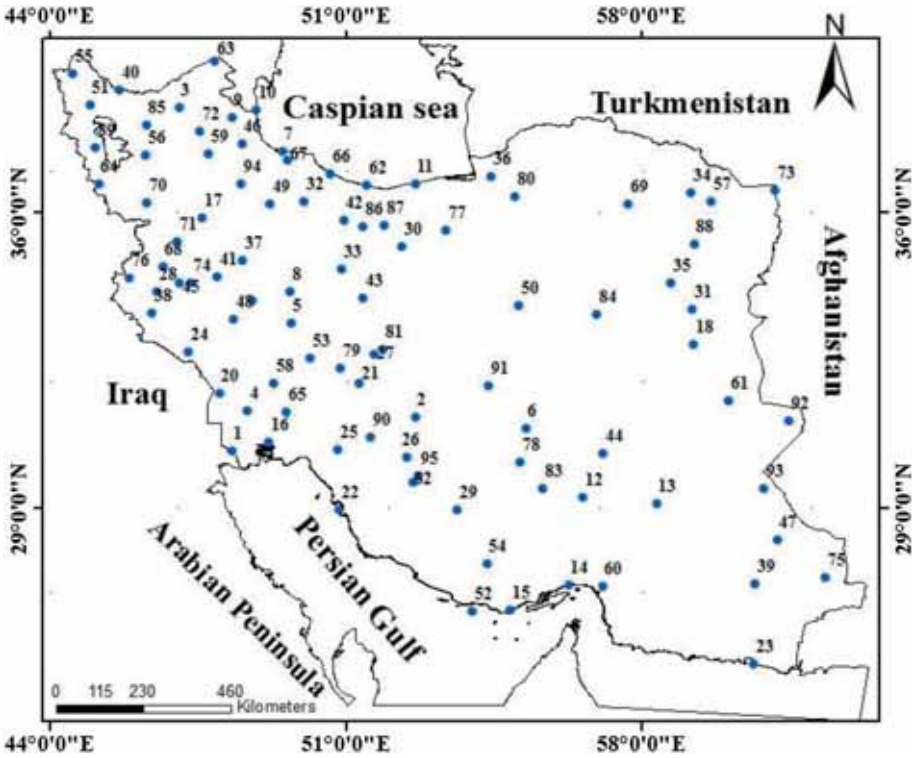

Figure 1. Spatial distribution of the selected synoptic stations in Iran.

temperature varying based on the proximity to primary water bodies and topography. January is usually the coldest month with average temperatures starting from 0° to 10°C. The hottest month is July with temperatures upwards of 20°–30°C (Soltani *et al.* 2016). In this study, stations with the longest duration of temperature collection, containing the fewest unavailable values were selected. These stations are scattered across the entire country. Clustering of minimal temperatures and their trends are performed primarily based on daily minimum temperatures.

2.2 *Data sets used in this study*

Clustering of frost frequencies and the trends of minimum temperatures from 1990 to 2015 were examined with a threshold much lower than 0°C, which is described as slight to moderate frost (0−1.5°C is slight frost and −1.5° to 3°C is moderate frost) and much lower than − 3°C is severe frost (Whiteman 1957; Rosenberg *et al.* 1983; Didari *et al.* 2012). Daily minimum temperatures recorded and operated by the Iran Meteorological Organization (IRIMO) at 95 synoptic stations over the period 1990–2015 were analysed. These synoptic stations have spread throughout the country in climatologically unique conditions (figure 1 and table 1). A disadvantage of all clustering algorithms is having a requirement of specifying the number of clusters into which each climate site is assigned through the analyses. These types of algorithms, including fuzzy clustering, are incapable of establishing the ideal number of clusters that best classify the sites climatologically (Irwin 2015). Therefore, for this purpose various cluster validation measures have been proposed in the literature. For identification of the optimal number of clusters, we have used five different cluster validation measures, namely, partition coefficient (PC), partition entropy (PE), modified partition coefficient (MPC), silhouette (SIL), fuzzy silhouette (SIL.F) and Xie and Beni (XB).

Also, annual trends of minimum temperatures were investigated for the stations of Clusters 1–5 from 1990 to 2015 with the aid of regression analysis. This study used the contemporary version, RClimDex, which runs in R, a language and environment for statistical computing. Threshold indices have been computed from 25 yr, 12-months base lengths for 1990–2015 to mirror the maximum current daily duration. There exist a total of 27 core extreme indices: 16 indices for temperature and 11 indices for precipitation. Temperature indices include nine warmth-related indices and seven cold-associated indices, and these may

Table 1. *Place names of analysed stations and their average annual frost frequencies with a threshold below 0° C and − 3° C over the period 1990–2015.*

Stations	Name	<0°C (days)	< −3°C (days)	Elevation (m)	Stations	Name	<0°C (days)	< −3°C (days)	Elevation (m)
1	Abadan	0.3	0	6.6	49	Khoram Dareh	90.3	52.2	1575
2	Abade	90.3	49.3	2030	50	Khor	23	5.6	845
3	Ahar	90.4	54.6	1390.5	51	Khoy	93	55.6	1103
4	Ahvaz	0.08	0	22.5	52	Kish	0	0	30
5	Aligudarz	92.4	52.6	2022	53	Kohrang	115	81.8	2285
6	Anar	55.4	26.6	1408.8	54	Lar	4	0.2	792
7	Anzali	1.5	0.2	− 26.2	55	Mako	93.3	63	1411.3
8	Arak	80.3	43.2	1708	56	Maragheh	71.4	40.4	1477.7
9	Ardabil	112	73	1332	57	Mashhad	61	25.8	999.2
10	Astara	11.7	1.3	− 18	58	Masjed Soleyman	0.3	0.08	320.5
11	Babolsar	1.5	0.04	− 21	59	Mianeh	78.6	45	1110
12	Baft	57.2	21.9	2280	60	Minab	0	0	29.6
13	Bam	4.3	0.8	1066.9	61	Nehbandan	32.9	10.3	1211
14	Bandar Abass	0	0	9.8	62	Noshahr	3.3	0.2	− 20.9
15	Bandar Lengeh	0	0	22.7	63	Pars Abad	45.6	14.5	31.9
16	Bandar Mahshahr	0.5	0	6.2	64	Piranshahr	68.2	39.3	1455
17	Bijar	91.8	56.5	1883.4	65	Ramhormoz	0.1	0	150.5
18	Birjand	73.3	39.8	1491	66	Ramsar	3.2	0.2	− 20
19	Brojerd	59.6	29.7	1629	67	Rasht	11.5	1.5	36.7
20	Bostan	2	0.08	7.8	68	Ravansar	64.5	29.7	1379.7
21	Boroojen	122.2	80.2	2197	69	Sabzevar	39.8	12.8	977.6
22	Bushehr Airport	0	0	19.6	70	Sagez	121.4	80.6	1522.8
23	Chabahar	0	0	8	71	Sanandaj	87.3	48.2	1373.4
24	Dehloran	0.3	0	232	72	Sarab	141	103.6	1682
25	Dogonbadan	2.4	0.08	699.5	73	Sarakhs	34.3	11.6	235
26	Drudzan	26.9	5.2	1620	74	Sararud	46.6	23.7	1361.7
27	Esfahan	65.7	29	1550.4	75	Saravan	10.7	1.6	1195
28	Eslam Abad	91.6	50.2	1348.8	76	Sarpol Zahab	15.4	2	545
29	Fassa	31	4.2	1288.3	77	Semnan	35	9.9	1130.8
30	Garmsar	41.2	14.2	825.2	78	Shahr Babak	87.9	52	1834.1
31	Ghaen	87.4	49.3	1432	79	Shahr Kord	128.3	88.4	2048.9
32	Ghazvin	80	41	1279.2	80	Shahrood	62.4	24.7	1345.3
33	Ghom	2.1	21.3	877.4	81	Shargh Esfahan	97.8	59.9	1543
34	Golmakan	79.4	38.8	1176	82	Shiraz	33.8	7.4	1484
35	Gonabad	45	15.5	1056	83	Sirjan	58	29	1739.4
36	Gorgan	16.45	1.88	13.3	84	Tabas	8.9	1.7	711
37	Hamadan Airport	106.8	69.8	1741.5	85	Tabriz	90.4	51.2	1361
38	Ilam	34.9	10.7	1337	86	Tehran	46.4	16	1548.2
39	Iranshahr	0.4	0	591.1	87	Tehran Airport	24.8	6.8	1190.8
40	Jolfa	74.8	42.6	736.2	88	Torbate Heydarieh	88.8	46.1	1450.8
41	Kangavar	101.4	58.6	1468	89	Urmia	107.2	63	1315.9
42	Karaj	56.9	26	1312.5	90	Yasuj	62.7	24	1831.5
43	Kashan	34.3	10.6	982.3	91	Yazd	31.6	9.1	1237.2
44	Kerman	77	44.3	1753.8	92	Zabol	18.7	5.6	489.2
45	Kermanshah	80	41.3	1318.6	93	Zahedan	44.6	21.4	1370
46	Khalkhal	136.2	92.6	1796	94	Zanjan	113	71.7	1663
47	Khash	22.3	6.2	1394	95	Zarghan	64.7	24.9	1596
48	Khoram Abad	52.4	18.4	1147.8	–	–			

Table 2. *List of the ETCCDI's seven cold-related indices and their definitions (available online at http://www.climdex.org/indices.html).*

Index	ID	Definition	Unit
Percentile			
Warm nights	TN90p	% of days when T_{min} is >90th percentile	%
Cool nights	TN10p	% of days when T_{min} is <10th percentile	%
Threshold			
Tropical nights	TR20	Annual count when T_{min}>20°C	days
Frost days	FD0	Annual count when T_{min}<0°C	days
Absolute			
Warmest night	TNx	Monthly maximum value of daily min temperature	°C
Coldest night	TNn	Annual minimum value of daily min temperature	°C
Cold spell duration	CSDI	Annual count of occurrences with at least 6 consecutive days when T_{min} < 10th percentile	°C

be further grouped in line with their methods of calculation as four percentile, four threshold, one absolute and three duration indices. In these observations, we used minimum temperature indices including seven cold-associated indices (table 2). Finally, the frost region and trends in extreme minimum temperature index maps are created in ArcGIS 10.1 by plotting the climate site locations and colour-coding them.

2.3 *Methodology*

2.3.1 *Fuzzy c-means algorithm*

Fuzzy clustering techniques primarily based on the goal characteristics are mostly examined by researchers and the most broadly used in practice. These rules take the clustering issue as a restrained optimisation problem, by the help of fixing the optimisation problem to decide the fuzzy partition and the clustering effects on the statistics set. Such algorithms are characterised by the help of simplification and smoothing applications, and the overall clustering performance is good, which can take the use of the classical optimisation principles as its theoretical guidance, making programming easier (Niu and Huang 2011). Bezdek and Dunn identified the simple concept of figuring out the fuzzy clusters by minimising an appropriately defined function, and have derived iterative algorithms for computing the membership functions for the clusters in the query (Bezdek 1981). By using the fuzzy-type approach, we are able to see that, depending on the degree of association of each item in unique clusters, how the station data partially or absolutely belong to the clusters (Das 2013). In recent years, advances in the fuzzy set research have spurred the improvement and application of fuzzy clustering techniques for a spread of programs in a one-of-a-kind discipline. On the other hand, the fuzzy c-approach (FCM) is a method of clustering which uses a single fact to associate data with two or more clusters to some degree that has specified a membership grade (Venkata Subbarao *et al.* 2013; Zeinali and Asghari 2016). This method is one of the commonly used fuzzy clustering techniques. It is based on the minimisation of the following objective feature:

$$J = (U, V) = \sum_{i=1}^{C} \sum_{j=1}^{N} u_{ij}^{m} \, d^2 \, (v_i, x_j) \quad (1 \leq m \leq \infty), \tag{1}$$

where m is the fuzziness parameter determining the level of cluster fuzziness, C is the number of clusters, n is the number of objects in the data set, v_i is the prototype of the centre of the cluster i, u_{ij} is the degree of membership of x_j in the cluster i and $d^2(v_i, x_j)$ is the distance between the object x_j and cluster centre v_i. V is a matrix including C cluster centres and U is a partition matrix. A solution of the object function can be obtained via a sequence of iterations, which is carried out as follows:

1. Set values for C (the number of clusters) and m (fuzziness parameter).
2. Initialise U (fuzzy partition matrix).
3. Calculate V (the cluster centres) by using U

$$v_i = \frac{\sum_{j=1}^{N} {u_{ij}}^m X_j}{\sum_{j=1}^{N} {u_{ij}}^m}. \tag{2}$$

4. Calculate the new partition matrix by using V

$$u_{ij} = \frac{1}{\sum_{k=1}^{c} \left(\frac{d(x_i, v_j)}{d(x_j, v_k)} \right)} 2/(m-1). \qquad (3)$$

5. Repeat steps 3 and 4 until the end condition is true (Izakian and Mesgari 2015).

Fuzzy c-means clustering is a frequently used and effective algorithm, but this technique also has some limitations such as the random selection of the midpoints means the iterative process often falls away from these midpoints. This may cause the clustering process to become less accurate. If the data sets contain substantial noise or are multidimensional, the process often fails to find the global optimum due to a poor clustering (Niu and Huang 2011; Zhang and Shen 2014). Another problem is that its prototypes run in the centre of data gravity, independent of prototype initialisation (Winkler *et al.* 2010).

2.3.2 *Extreme indices calculation*

Interest in global warming is changing from analysis of normal values to increasing expertise and reading in the outcomes of extremes. Because of the very nature of extreme events being rare, corresponding statistical assessments are loaded with uncertainty (Bürger *et al.* 2012). The ClimDEX indices are recommended by using the IRIMO's expert team on climate change detection and indices (ETCCDI) as a method of summarising each day's temperature and precipitation statistics, focusing particularly on aspects of climate extremes (Werner and Cannon 2016). It has a core set of 27 indices: the 27 core indices consist of 16 temperature and 11 precipitation indices. Temperature indices include nine heat-associated indices and seven cold-associated indices, and those may be further grouped in line with their approach of calculation as four percentile, four threshold, one absolute and three period indices (Powell and Keim 2015). Minimum temperature indices consisting of seven cold-related indices had been chosen for the present examination (table 2). The indices were calculated with the help of the computer application RClimDex, which is an open-source software (http://cccma.Seos.Uvic.Ca/ETCCDI/software_program.shtml), affiliated with the R platform (http://www.R-venture.org/). RClimDex performs the index calculations using daily statistics and gives monthly and yearly statistics. It includes fine data management, which became useful to construct the database used on this examination (López-Díaz *et al.* 2013). The RClimDex program makes use of linear regression for trend calculations. The RClimDex software program produces time series and computes trends by way of linear least-squares and locally weighted linear regression using a less smoother feature in R (Zhang and Yang 2004).

3. Results and discussion

The optimal number of clusters generally varies between 2 and the square root of the number of total data points (Goyal and Gupta 2014; Gupta and Goyal 2015). Therefore, we have computed various validation measures for the cluster numbers varying from 2 to 10. Figure 2 shows the results of the validation measures obtained for fuzzy c-means clustering algorithm for the number of clusters varying from 2 to 10.

As it can be observed from figure 2, the partition entropy (PE) has been found to be having monotonic trends; thus, it can be considered ineffective in identifying the optimum number of clusters. The minimum value of Xie and Beni (XB) index reflects the optimum well-separated number of clusters; thus, the XB index was found to have the minimum value for the number of clusters to be 4 and 5. The maximum value of PC and MPC indices reflects the optimum number of clusters for the highest values. PC was found to be at maximum for 2 clusters, but considering the two clusters will not cover the heterogeneity in such a large area, they cannot be considered. The second highest value of PC was found for five clusters. For MPC, nine clusters were found to be showing an optimum number but after visualising the formed clusters, it was found that it was forming some very small clusters; thus, according to this index, 5 or 6 can be considered as an optimum number for the well-separated clusters. The silhouette index was found to be showing four clusters as optimum. Since all indices were showing a different number as the optimum number, the cluster number 5 was selected which agrees with the most number of indices. Climate sites were therefore divided into five homogeneous clusters by frost period and duration over Iran. Cluster 5 was very large and physically heterogeneous; thus, it is appropriate to divide it into three subregions. Thus, Cluster 5 was further divided into three separate clusters using fuzzy c-means

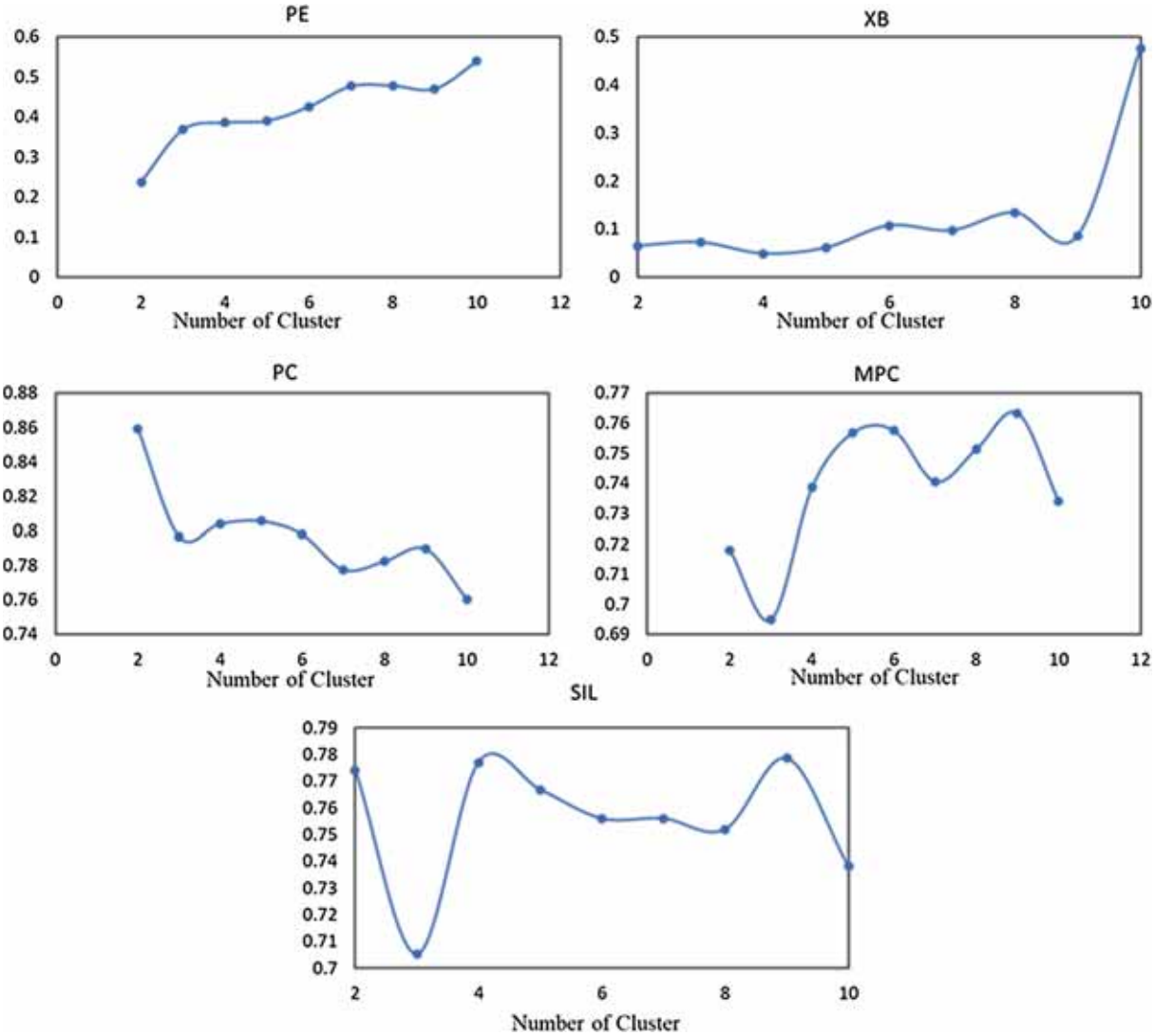

Figure 2. Cluster validation measures varying from 2 to 20 clusters.

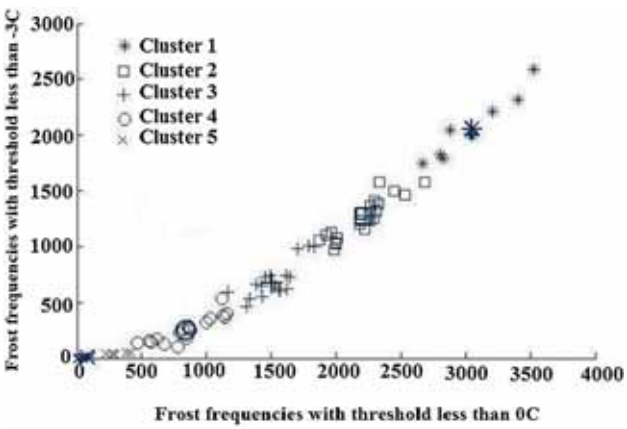

Figure 3. Clustered data set by using the fuzzy c-means algorithm.

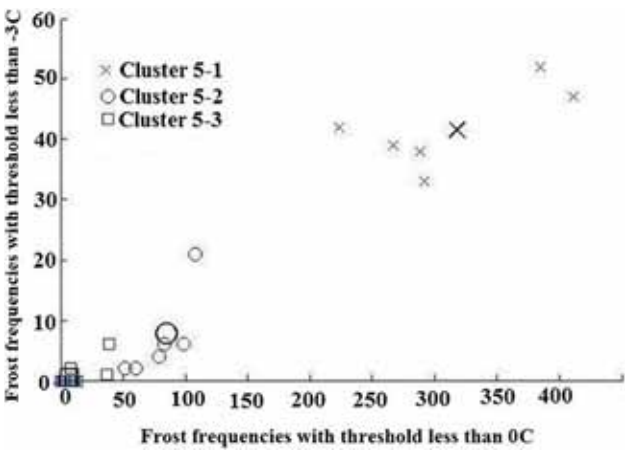

Figure 4. Re-clustering of Cluster 5 set by using the fuzzy c-means algorithm.

clustering algorithm. The process of clustering was found to be doing a good job in dividing the country into climatic zones based on frost data.

The FCM clustering was undertaken on the frost frequencies with a threshold less than 0°C and -3°C from 1990 to 2015 and are presented

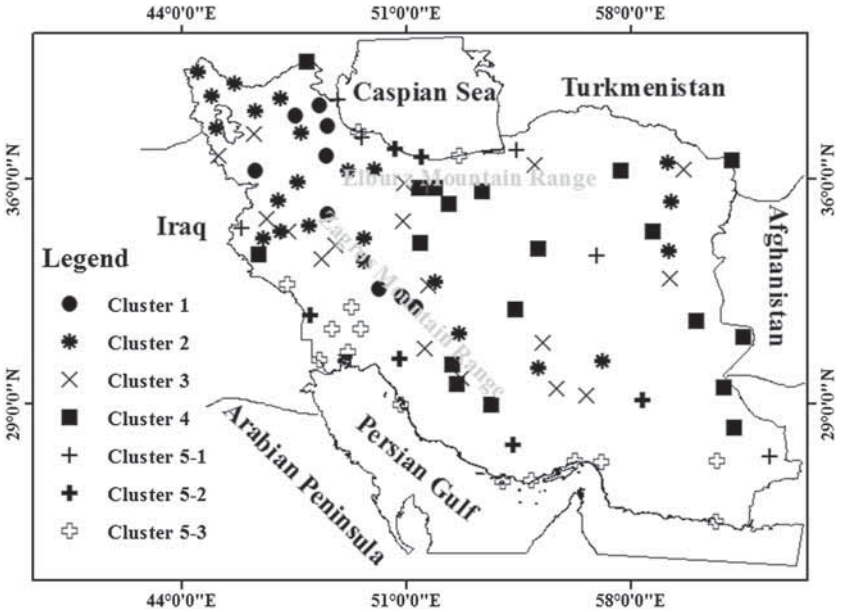

Figure 5. Location of fuzzy clusters obtained using the fuzzy clustering analysis.

in table 1. The entire region was divided into five subregions according to two extracted indices (figure 3).

Cluster 5 includes stations which encompass the north and south of the country, which was changed into a reclassification into three subgroups (figure 4). Discerning the three subgroups is suggested for the reclassification of the stations of this group. In consistency with this clustering (figure 5), the greatest frost frequencies belong to the high altitude regions of the country, consisting of Ardabil, Khalkhal, Sarab, Zanjan, Saghez and Hamadan Airport (northwest Iran); Shahr kord, Boroojen and Kohrang (southwest Iran) (figure 1), all in Cluster 1, and are located within the western half of Iran. For this reason, one can conclude that the frost frequency is influenced by elevation and in mountainous areas. In this cluster, Sarab station has the greatest annual frequency of frost at 141.1 days over the 1990–2015 period, with a height of 1680 m, and Hamadan Airport station has the lowest frequency of frost at 106.8 days over the 25-yr period. Cluster 2 contains Tabriz, Mianeh, Jolfa, Ahar, Urmia, Mako, Khoy and Khoram Dareh (northwest Iran); Kermanshah, Eslam Abad, Kangavar, Sanandaj and Bijar (west Iran); Shargh Esfahan, Shahr Babak, Arak, Abadeh, Kerman and Ghazvin (central Iran); Aligudarz (southwest Iran); Golmakan, Torbate Heydariyeh and Ghaen (northeast Iran), located throughout Iran and at high elevation and in mountainous areas. Their annual frost frequencies vary from 74.8 to 107.2 days over the 25-yr study period. The greatest frequency of frosts in this cluster belongs to Urmia and the lowest frequency belongs to the station of Jolfa. Cluster 3 includes Maragheh and Piranshahr (northwest Iran); Esfahan, Zarghan, Ghom, Baft, Sirjan, Anar and Karaj (central Iran); Ravansar and Sararud (western Iran); Mashhad and Shahrood (northeast Iran); Birjand (eastern Iran) and Brojerd, Khoram Abad and Yasuj (southwest Iran). This cluster has annual frost frequencies of 46.6–73.3 days over the study period. The lowest and greatest frost frequencies observed were at the Brojerd and Esfahan stations, respectively. Cluster 4 incorporates the stations Pars Abad (northwest Iran); Sarakhs, Sabzevar and Gonabad (northeast Iran); Nehbandan, Zabol and Zahedan (eastern Iran); Khor, Kashan, Shiraz, Drudzan, Fassa, Yazd, Tehran Airport, Tehran, Semnan and Garmsar (central Iran); Khash (southeast Iran) and Ilam (western Iran). In this cluster, the greatest and the lowest annual frost frequencies determined were at Tehran (46.4 days) and Zabol (18.7 days), respectively. In all, Clusters 1–4 represent stations that spread throughout the country. The exceptions are coastal areas in the north and south of Iran. In these stations, the Siberian and European migratory high-pressure systems play a critical function; that is, while these systems dominate over Iran, cold weather enters the country from the west, northwest and the northeast, causing cold weather in those areas.

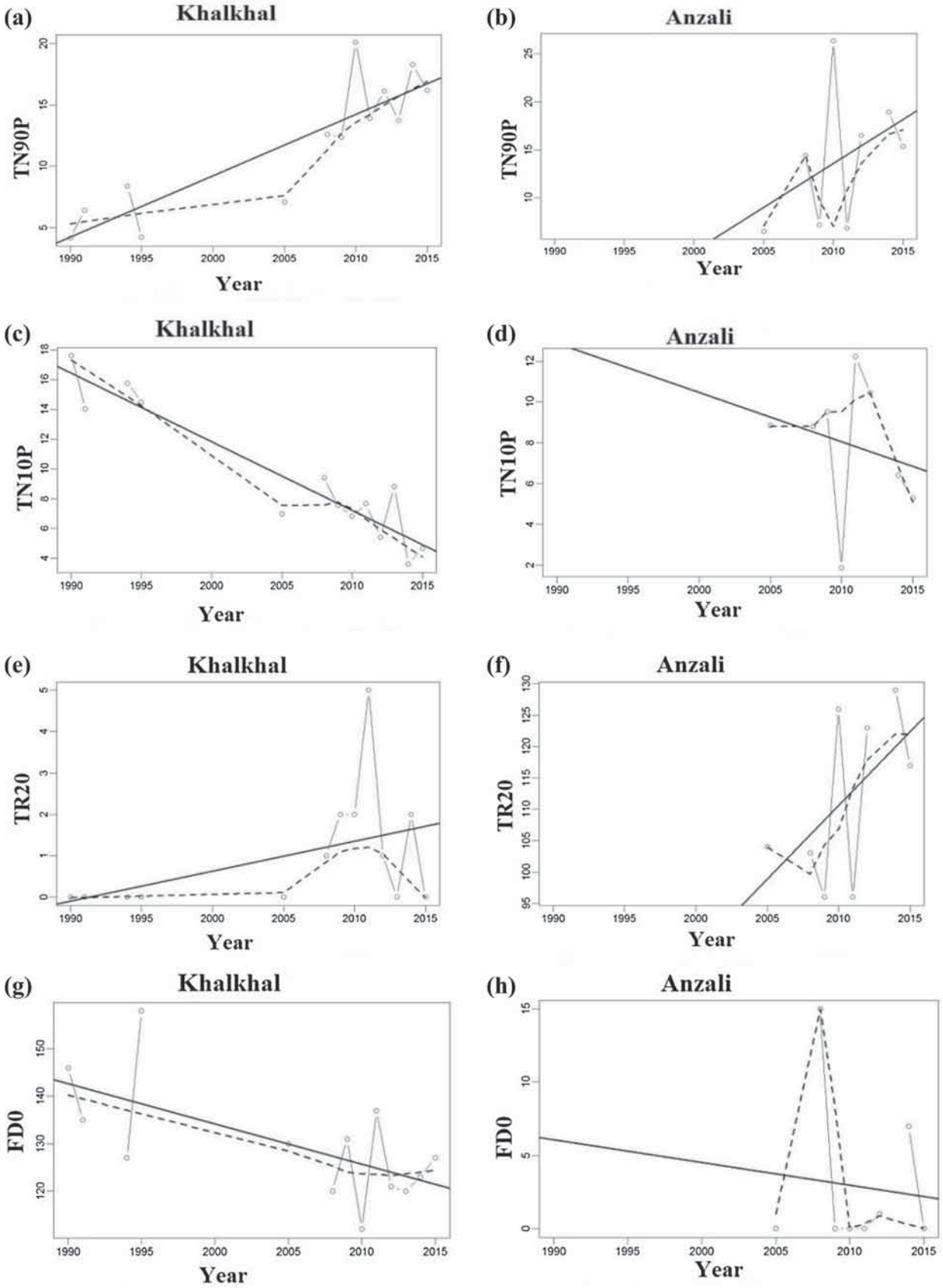

Figure 6. Evolution of warm nights (TN90p), cool nights (TN10p), tropical nights (TR20), frost days (FD0), warmest night (TNx), coldest night (TNn) and cold spell duration (CSDI) for two selected stations in Iran from 1990 to 2015. Khalkhal (**a**, **c**, **e**, **g**, **i**, **k**, **m**) and Anzali (**b**, **d**, **f**, **h**, **j**, **l**, **n**).

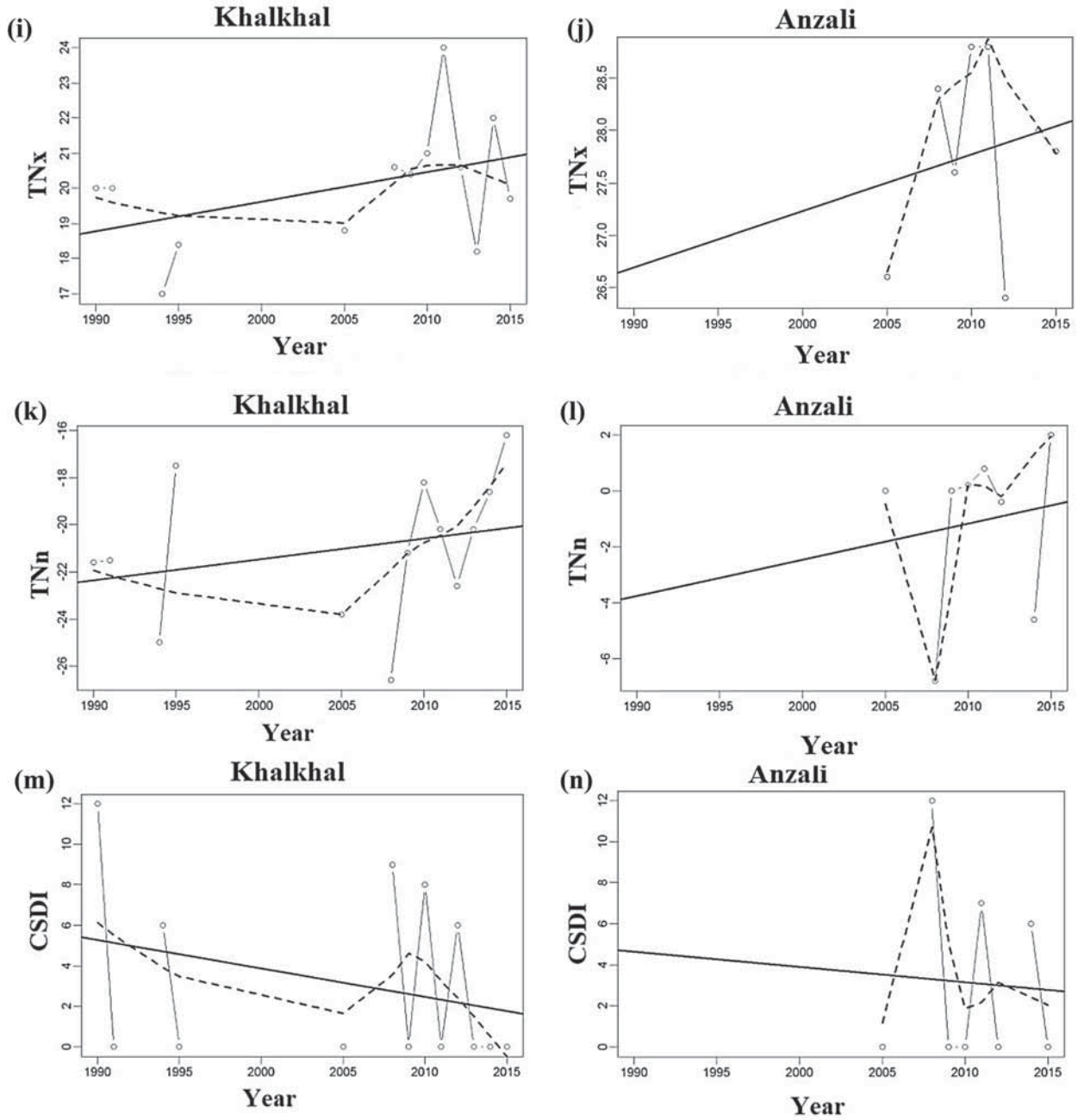

Figure 6. (*Continued.*)

Clusters 5–1, 5–2 and 5–3 consist of the coastal regions of Iran which are located next to the Persian Gulf in the south and the Caspian Sea in the north. Along the north coast of the country, because of the humidity from the Caspian Sea and some elevation and along the south coast of the country, particularly, the coast of the Persian Gulf, due to the low latitude and the dynamic influence of subtropical high-pressure systems, fewer cold waves and frosts are experienced. The average annual frost frequency in these clusters is between 0 and 16.4 days. Stations placed in each of these clusters (Cluster 5 subgroups) are not homogeneous in terms of geographical position, climate and frost occurrence; however, but are homogeneous in terms of severity and frequency of frosts. Normally, the frequency of frost increases as one goes from the lowlands and lower elevations of the south and north of Iran toward the high elevations of the Zagros and Elburz mountains and the northwest, southwest and northeast of Iran (figure 5). This is directly related to elevation and location of these

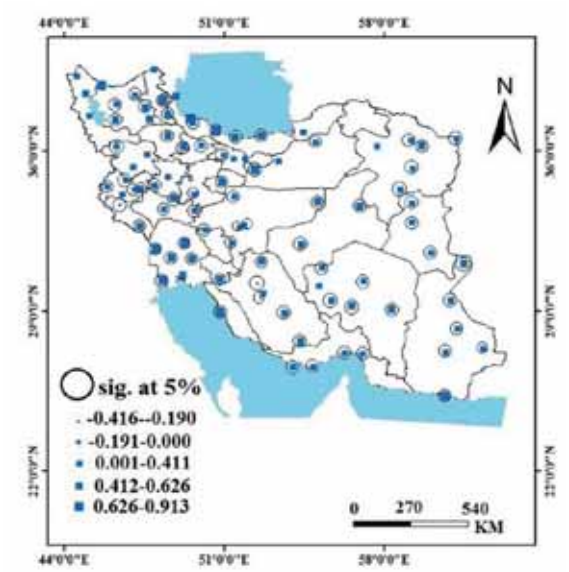

(a) Warm nights, 1990–2015. % of days when Tmin is >90th percentile

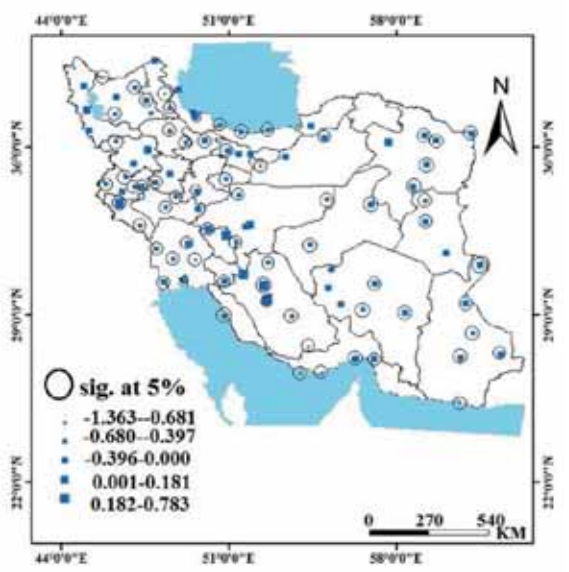

(b) Cool nights, 1990–2015. % of days when Tmin is <10th percentile

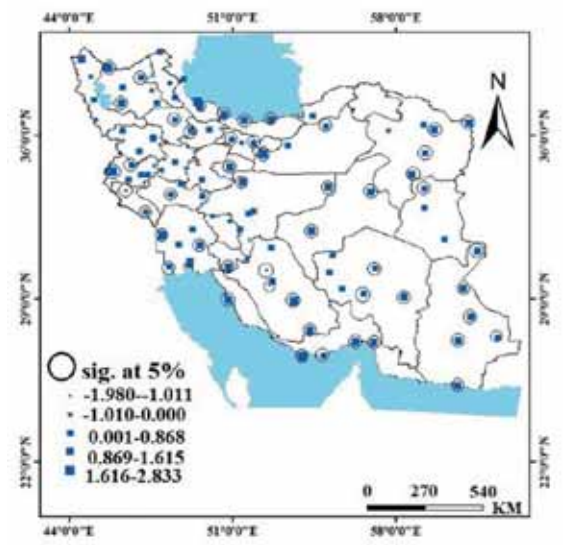

(c) Tropical nights, 1990–2015. Annual count when Tmin >20°C

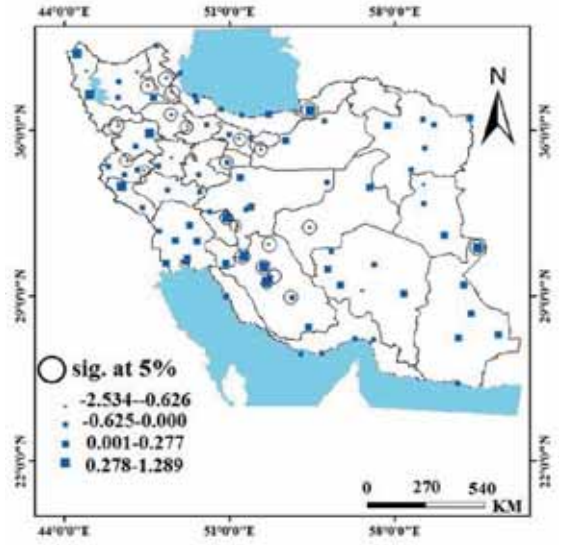

(d) Frost days, 1990–2015. Annual count when Tmin <0°C

Figure 7. Trends in extreme minimum temperature indices for Iran from 1990 to 2015. The circles are significant at the 0.05 level.

stations, their situation in the position of external synoptic systems, physical and geomorphological functions and local weather.

Mahmoudi (2014) showed that temperatures over highland areas which reach up to 4200 m above the sea level were always greater than 0°C or below 0°C at some point of the year and, additionally, the coastal zone of southern Iran had no frost. Elevation becomes the main factor for the frequency of frost incidence.

Daily minimum temperature-related indices show a common warming trend at some stage in Iran for the period from 1990 to 2015 (figure 7). Certainly, if one examines the frequency of cool nights (figure 6c and d), it appears that the maximum from these stations shows a negative slope varying from -1.365 to -0.5, which means that the nights have become warmer and warm nights display a positive slope, apart from a few stations, varying from 0 to 0.913, which shows that warm nights have become more frequent (figure 6a and b). The tropical night range indicates a positive trend (figure 6e and f). Given that minimum temperatures have increased over the period,

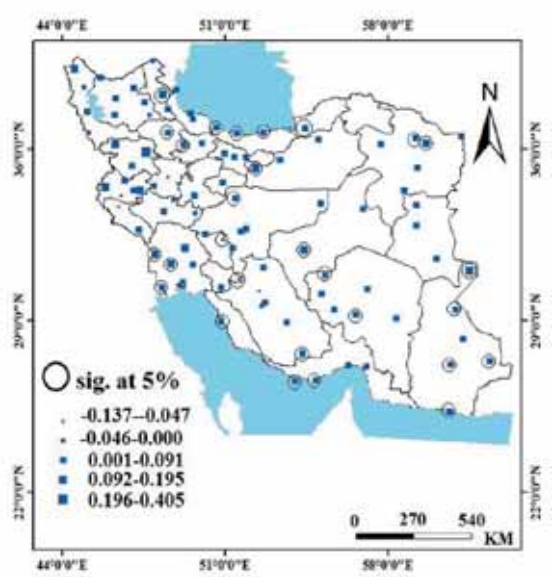

(e) Warmest nights, 1990–2015. Monthly maximum value of daily min temperature

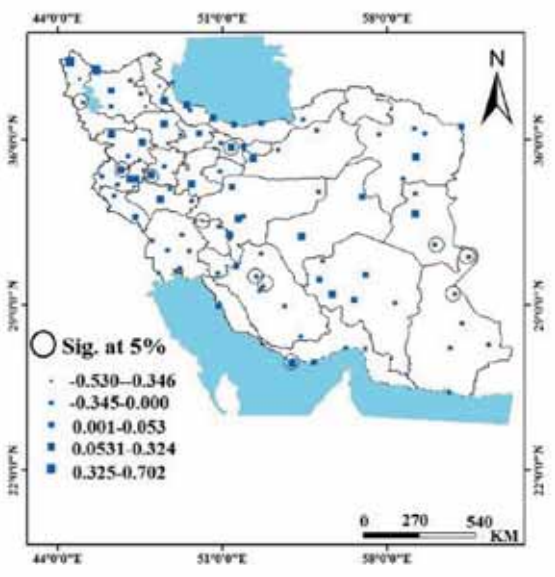

(f) Coldest nights, 1990–2015. Annual minimum value of daily min temperature

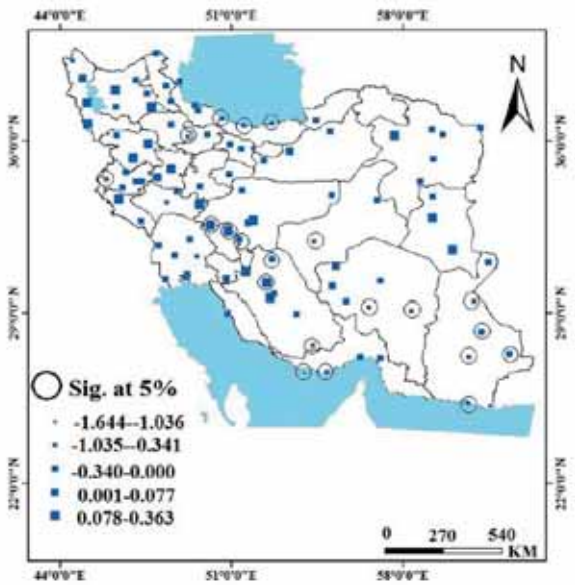

(g) Cold spell duration, 1990–2015. Annual count of occurrences with at least 6 consecutive days when Tmin <10th percentile

Figure 7. (*Continued.*)

figure 6 illustrates that, from the selected stations, a consistent warming has occurred throughout the study period. Indeed, while the frequency of cool nights, frost days (figure 6g and h) and cold spells (figure 6m and n) have decreased, that of warm nights and tropical nights have increased. There are no cooling trends throughout for the 5% level. About 93% of stations showed an increase in warm nights, and 78% of stations are significant. Approximately, 88% of stations showed a decrease in cool nights, with 78% being significant. About 89% of stations showed an increase in tropical nights, and 59% of stations are significant. The warming trend for frost days is vast at the 5% level for 22% (65%) of all 95 stations analysed. About 86% and 41% of stations showed an increase in the warmest nights (figure 6i and j) and the coldest nights (figure 6k and l), with 29% and 11% being significant, respectively. The warming trend for the cold spell length is significant for 21% (73%) of the 95 stations.

Ultimately, the annual characteristics have been mapped to observe spatial modes in these indices

across Iran. Spatial traits in the minimum-temperature associated indices are shown in figure 7. Blue squares show variations from small to large, constituting a slope. The smallest rectangles represent negative slopes and the largest ones represent positive slopes in the direction of a hotter climate. Circles suggest significance at the 5% level. Most stations experienced upward trends in extreme minimum temperatures. Most places showed upward trends in warm nights above the 90th percentile (figure 7a), with some exceptions in northwest Iran. Further evidence of nighttime warming changes are determined using cool nights (figure 7b), excluding central and northwest Iran. Similarly, region-wide increasing trends have been discovered in the index for tropical nights, with many trends significant at the 5% level (figure 7c). Conversely, frost days have been decreasing for most stations (figure 7d). Figure 7(e) shows vicinity-wide increases in the warmest nights, with some trends significant at 5%. A few indices confirmed much less spatial coherence and exhibited fewer widespread trends, together with the coldest nights (figure 7f). Figure 7(g) shows region-wide decreases in cold spell duration, with some traits significant at 5%. Preceding studies in Iran confirmed the same trends in minimum temperature indices that we found. For instance, Parak *et al.* (2015) and Soltani *et al.* (2016) showed strongly positive tendencies over past decades in tropical night and warm night indices, and decreasing trends were found for frost days, cool nights and cold spell duration indices over most regions of Iran.

4. Conclusions and recommendations

Frost is a major climatological phenomenon affecting different regions in various ways, over different latitudes, and annually causes damaging losses in various sectors directly or indirectly. Therefore, the identification and clustering of this phenomenon is essential and is a priority in climate studies. According to these results, Iran is classified in five clusters by frost frequency, from which Cluster 5 is reclassified in three subgroups because of its wide range. Locations of the greatest frost occurrences are Ardabil, Khalkhal, Sarab, Zanjan, Sagez and Hamadan Airport (northwest Iran); Shahr kord, Boroojen and Kohrang (southwest Iran) stations (Cluster 1); Tabriz, Mianeh, Jolfa, Ahar, Urmia, Mako, Khoy and Khoram Dareh (northwest Iran); Kermanshah, Eslam Abad, Kangavar, Sanandaj and Bijar (western Iran); Sharg Esfahan, Shahr Babak, Arak, Abadeh, Kerman and Ghazvin (central Iran); Aligudarz (southwest Iran); Golmakan, Torbate Heydariyeh and Ghaen (northeast Iran) (Cluster 2); Maragheh and Piranshahr (northwest Iran); Esfahan, Zarghan, Ghom, Baft, Sirjan, Anar and Karaj (central Iran); Ravansar and Sararud (western Iran); Mashhad and Shahrood (northeast Iran); Birjand (eastern Iran); Brojerd, Khoram Abad and Yasuj (southwest Iran) (Cluster 3), with an average annual frost frequency between 46.6 and 73.3 days over the 25-yr study period. Locations with the lowest frost frequencies are in Clusters 5–1, 5–2 and 5–3, including the coastal regions of Iran which are located along the Persian Gulf in the south and the Caspian Sea in the north, experiencing between 0 and 16.4 days of frost annually over the 25-yr study period. Generally, the frequency of frost increases from the lowlands and the lower elevations of the south and north coasts of Iran toward the higher elevations of the Zagros and Elburz mountains and the northwest, southwest and northeast of Iran. This is directly related to the elevation and latitude of these stations, their locations in the path of external synoptic systems, physical and geomorphological features and local climate. Also, in this study, we analysed annual changes in extreme minimum temperature indices within the period 1990–2015 over Iran by using a data set of seven daily minimum temperature series. Trends of daily minimum temperatures were investigated for all stations using RClimDex. This study showed that throughout Iran, the minimum temperature indices show a general warming trend since 1990. There are positive trends at the 0.05 significance level for most stations in warm nights, tropical nights, warmest nights and coldest nights. There are also negative trends in cool nights, frost days and cold spell duration that are related to global warming.

The results also suggest the need for further investigation into greenhouse gases emissions into the atmosphere, especially for industrial areas, which could be one of the major causes of climate change in Iran. Homogeneous climatic element areas are frequently used in climate projection applications (Steinhaeuser *et al.* 2011; Badhiye *et al.* 2012; Bador *et al.* 2015; Kumar and Swamy 2015). Results show more accurate projections over uniform areas than extensive heterogeneous zones (Irwin 2015). According to that, the results of the

current work could be used to forecast climate changes using different general circulation model (GCM) data.

Acknowledgements

The authors would like to thank the I.R. of Iran Meteorological Organisation (IRIMO) for providing the meteorological data for this study. We also would like to thank Stephen Berg for assistance with the writing. We also acknowledge financial support from Mohaghegh Ardabili University.

References

Amer M and Wang C 2017 Review of defrosting methods; *Renew. Sust. Energ. Rev.* **73** 53–74.

Badhiye S S, Chatur P N and Wakode B V 2012 Temperature and humidity data analysis for future value prediction using clustering technique: An approach; *Int. J. Emerg. Technol. Adv. Eng.* **2**(**1**) 88–91.

Bador M, Naveau P, Gilleland E, Castellà M and Arivelo T 2015 Spatial clustering of summer temperature maxima from the CNRM-CM5 climate model ensembles & E-OBS over Europe; *Weather Clim. Extrem.* **9** 17–24.

Bezdek J C 1981 *Pattern recognition with fuzzy objective function algorithms*; Plenum Press, New York, 256p.

Bürger G, Murdock T Q, Werner A T, Sobie S R and Cannon A J 2012 Downscaling extremes – An intercomparison of multiple statistical methods for present climate; *J. Clim.* **25**(**12**) 4366–4388.

Crimp S J, Gobbett D, Kokic Ph, Nidumolu U, Howden M and Nicholls N 2016 Recent seasonal and long-term changes in southern Australian frost occurrence; *Clim. Change* **139**(**1**) 115–128.

Das S 2013 Pattern recognition using the fuzzy c-means technique; *Int. J. Energy Res. Inf. Commun.* **4**(**1**) 1–14.

Didari Sh, Zand-Parsa Sh, Sepaskhah A R, Kamgar-Haghighi A A and Khalili D 2012 Preparation of frost atlas using different interpolation methods in a semiarid region of south of Iran; *Theor. Appl. Climatol.* **108**(**1–2**) 159–171.

Ghasemi A R and Khalili D 2006 The influence of the Arctic oscillation on winter temperature in Iran; *Theor. Appl. Climatol.* **85** 149–164.

Ghasemi A R and Khalili D 2008 The effect of the north Sea Caspian pattern on winter temperatures in Iran; *Theor. Appl. Climatol.* **92** 59–74.

Goyal M K and Gupta V 2014 Identification of homogeneous rainfall regimes in northeast region of India using fuzzy cluster analysis; *Water Resour. Manag.* **28**(**13**) 4491–4511.

Gupta V and Goyal M K 2015 Impact of climate change on regionalization using fuzzy clustering; In: *Proceedings of fourth international conference on soft computing for problem solving*, Springer, New Delhi, pp. 455–462.

Hartmann D L, Klein Tank A M G, Rusticucci M, Alexander L V, Brönnimann S, Charabi Y, Dentener F J, Dlugokencky E J, Easterling D R, Kaplan A, Soden B J, Thorne P W, Wisld M and Zhai P M 2013 Observations: Atmosphere and surface; In: *Climate change 2013: The physical science basis. Contribution of working group I to the fifth assessment report of the intergovernmental panel on climate change* (eds) Stocker T F, Qin D, Plattner G-K, Tignor M, Allen S K, Boschung J, Nauels A, Xia Y, Bex V and Midgley P M, Cambridge University Press, Cambridge, UK and New York, NY.

Hejazizadeh Z and Naserzadeh M H 2007 Calculation and analysis of frost duration times by using Delphi programming: A case study in Lorestan, Iran; *J. Appl. Sci.* **7** 3831–3835.

Hernandez A R and Martinez L R 2009 The risk of early and late frost behavior in central Mexico under El Nino conditions; *Atmosfera* **22**(**1**) 111–123.

IPCC 2013 Climate change 2013: The physical science basis; In: *Contribution of working group I to the fifth assessment report of the intergovernmental panel on climate change* (eds) Stocker T F, Qin D, Plattner G-K, Tignor M, Allen S K, Boschung J, Nauels A, Xia Y, Bex V and Midgley P M, Cambridge University Press, Cambridge, UK and New York, NY, USA, 1535p.

Irwin S E 2015 Assessment of the regionalization of precipitation in two Canadian climate regions: A fuzzy clustering approach; MS Thesis, The University of Western Ontario.

Izakian Z and Mesgari M S 2015 Fuzzy clustering of time series data: A particle swarm optimization approach; *J. AI Data Min.* **3**(**1**) 39–46.

Kumar A and Swamy A K 2015 Comparison of clustering approaches on temperature zones for pavement design; In: *Bituminous mixtures and pavements VI*, 211p.

López-Díaz F, Conde C and Sánchez O 2013 Analysis of indices of extreme temperature events at Apizaco, Tlaxcala, Mexico: 1952–2003; *Atmosfera* **26**(**3**) 349–358.

Mahmoudi P 2014 Mapping statistical characteristics of frosts in Iran; *Int. Arch. Photogramm. Remote Sens. Spat. Inf. Sci.* **40**(**2**) 175.

Mouhamed L, Traore S B, Alhassane A and Sarr B 2013 Evolution of some observed climate extremes in the West African Sahel; *Weather Clim. Extrem.* **1** 19–25.

Niu Q and Huang X 2011 An improved fuzzy C-means clustering algorithm based on PSO; *J. Softw.* **6**(**5**) 873–879.

Parak F, Roshani A and Jamali J B 2015 Trends and anomalies in daily climate extremes over Iran during 1961–2010; *J. Environ. Agric. Sci.* **2**(**11**) 1–17.

Powell E J and Keim B D 2015 Trends in daily temperature and precipitation extremes for the Southeastern United States: 1948–2012; *J. Clim.* **28** 1592–1612.

Rosenberg N J and Myers R E 1962 The nature of growing season frosts in and along the Platte Valley of Nebraska; *Mon. Weather Rev.* **90(11)** 471–476.

Rosenberg N J, Blad B L and Verma S B 1983 *Microclimate: The biological environment*; John Wiley & Sons, New York, 495p.

Soltani M, Laux P, Kunstmann H, Stan K, Sohrabi M M, Molanejad M, Sabziparvar A A, Ranjbar SaadatAbadi A, Ranjbar F, Rousta I, Zawar-Reza P, Khoshakhlagh F, Soltanzadeh I, Babu C A, Azizi G H and Martin M V 2016 Assessment of climate variations in temperature and precipitation extreme events over Iran; *Theor. Appl. Climatol.* **126**(**3–4**) 775–795.

Steinhaeuser K, Chawla N V and Ganguly A R 2011 Comparing predictive power in climate data: Clustering matters; In: *International symposium on spatial and temporal databases*; Springer, Berlin, Heidelberg, pp. 39–55.

Tamandani B K, Mahmood Khosravi D and Mahmoodi P 2015 Mapping and analyzing the risk of frost and chilling damage on horticultural crops (study case: Taftan border area, Southeast of Iran); *J. Bio. Environ. Sci.* **7**(**2**) 261–275.

Vega A J, Robbins K D and Grymes J M 1994 Frost/freeze analysis in the Southern Climate Region; Report No. 1, Southern Regional Climate Center, 388p.

Venkata Subbarao M, Sayedu Khasim N, Thati J and Sastry M H H 2013 Non-stationary power quality signals classification using fuzzy C-means algorithm; *Int. J. Adv. Res. Comput. Eng. Technol.* **2**(**2**) 812–816.

Werner A T and Cannon A J 2016 Hydrologic extremes – An inter comparison of multiple gridded statistical downscaling methods; *Hydrol. Earth Syst. Sci.* **12** 6179–6239.

Whiteman T M 1957 Freezing points of fruits, vegetables and florist stocks; U.S. Dept. of Agric. Marketing Res. Report. No. 196, 32p.

Winkler R, Klawonn F and Kruse R 2011 Fuzzy c-means in high dimensional spaces; *Int. J. Fuzzy Syst.* **1**(**1**) 1–16.

Zeinali B and Asghari S 2016 Mapping and monitoring of dust storms in Iran by fuzzy clustering and remote sensing techniques; *Arab J. Geosci.* **9**(**549**) 1–10.

Zhang X and Yang F 2004 *RClimdex (1.0) user manual*; Climate Research Branch Environment Canada Downsview, Ontario, Canada, 23p.

Zhang J and Shen L 2014 An improved fuzzy c-means clustering algorithm based on shadowed sets and PSO; *Comput. Intell. Neurosci.* **2014** 22.

Corresponding editor: N V Chalapathi Rao